Elastic and Inelastic Photon-Scattering Studies at HIγS

G. Rusev

Department of Physics, Duke University

Triangle Universities Nuclear Laboratory

Workshop on Gamma Strength and Level Density in Nuclear Physics
Nuclear Technology

Aug. 30, 2010

Outlook

- High-Intensity γ-ray Source.
- Photon-scattering experiments on ^{90}Zr and ^{98}Mo.
  - $E1$ and $M1$ strength distributions.
  - Branching ratios for transitions to the ground state.
  - Photoabsorption cross section.
- Tail of the GDR in ^{138}Ba.
- Elastic photon scattering from ^{235}U.

High-Intensity γ-ray Source (HIγS)

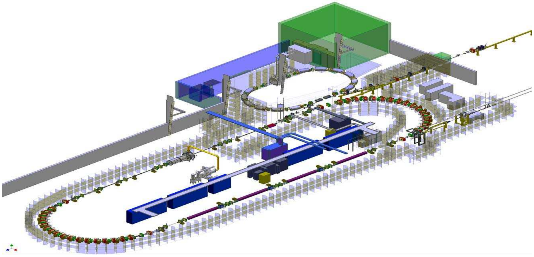

- 260 MeV electron accelerator
- 1.2 GeV storage ring
- Booster
- 2 free-electron lasers
- 1 – 100 MeV photon beams
- 0.5 – 5% energy spread
- linear or circular polarization

Inverse Compton scattering

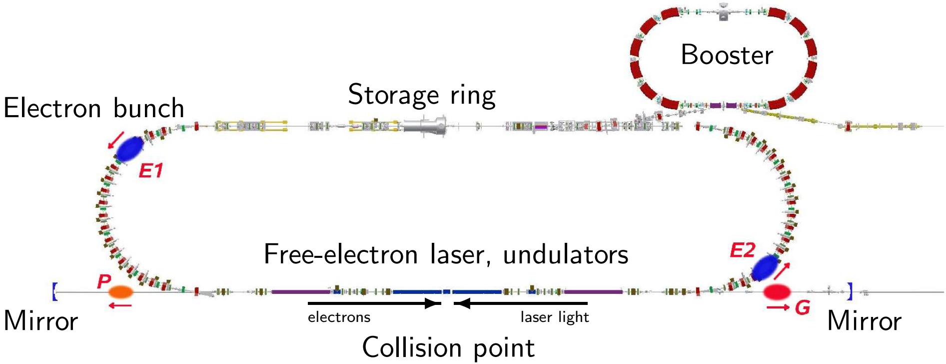

Inverse Compton scattering

Compton scattering

$$E_\gamma \approx \frac{4\gamma^2 E_p}{1+\gamma^2\theta_f^2+4\gamma^2 E_p/E_e}$$

$$\gamma = 1/\sqrt{1-\beta^2}$$

C. Sun *et al.*, Phys. Rev. ST Accel. Beams **12**, 062801 (2009)

Elec

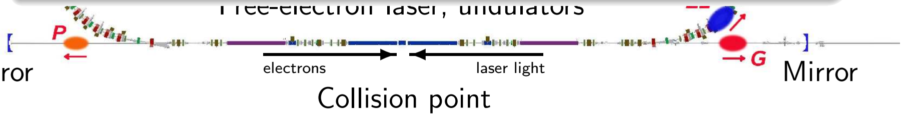

Inverse Compton scattering

Compton scattering

$$E_\gamma \approx \frac{4\gamma^2 E_p}{1+\gamma^2\theta_f^2+4\gamma^2 E_p/E_e}$$

$$\gamma = 1/\sqrt{1-\beta^2}$$

C. Sun *et al.*, Phys. Rev. ST Accel. Beams **12**, 062801 (2009)

Elec

Free-electron laser, undulators

Mir

r

Photon-beam properties

Monochromaticity

Linearly polarized

Spin and Parity Determination

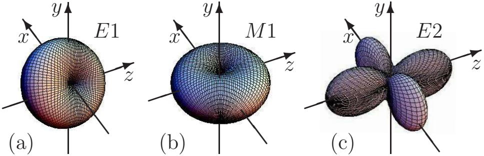

z axis: beam direction; x axis: vector of polarization

Angular distribution

Measurement of the transition intensity at three different angles allows unique assignment of the e.m. character and multipolarity of the transition.

Spin and Parity Determination

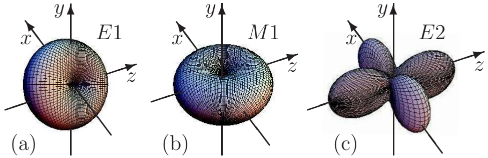

z axis: beam direction; x axis: vector of polarization

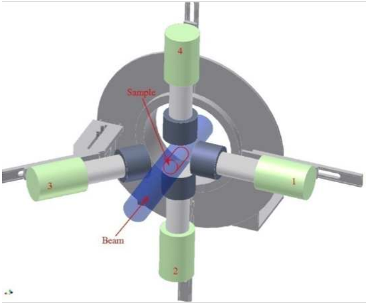

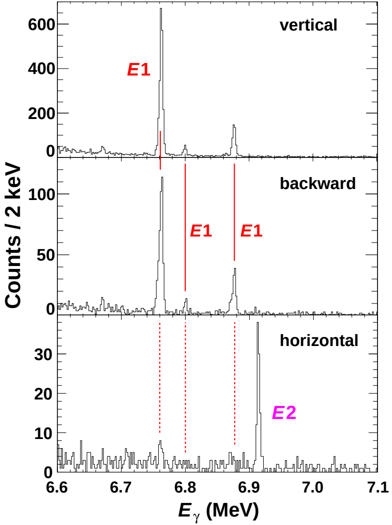

Spin and Parity Determination

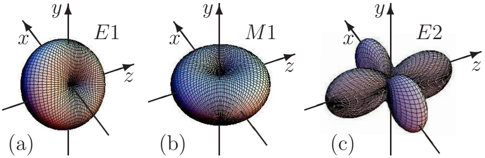

z axis: beam direction; x axis: vector of polarization

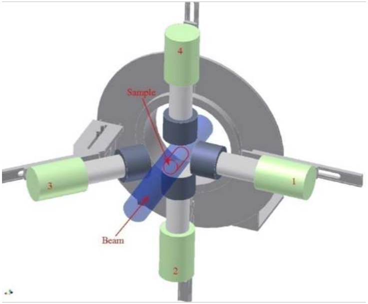

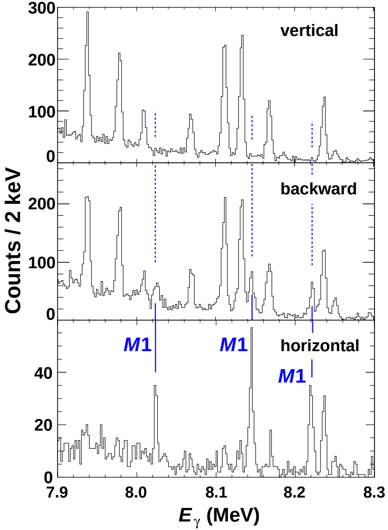

Giant $M1$ Resonance in ^{90}Zr

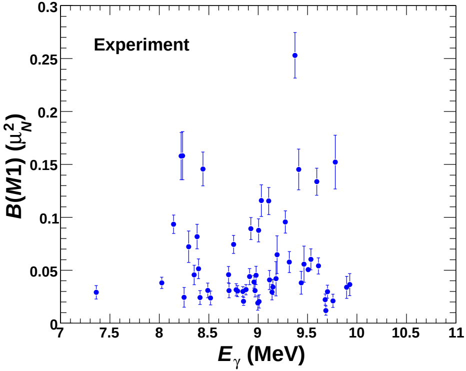

G. Rusev *et al.*, Phys. Rev. Lett. (2010), to be submitted

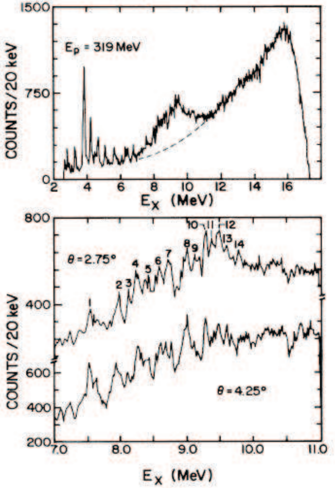

S. K. Nanda *et al.*, Phys. Rev. Lett. **51**, 1526 (1983)

Measurement of the Beam-Energy Distribution

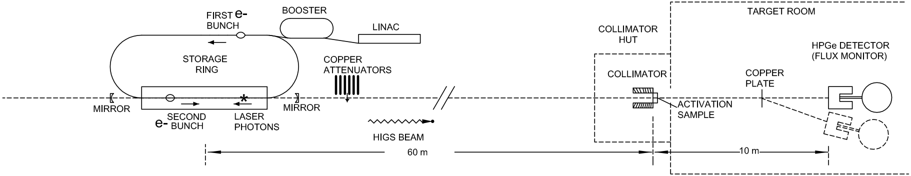

- Large volume HPGe detector
- Cu attenuators placed 40 m away from the HPGe detector

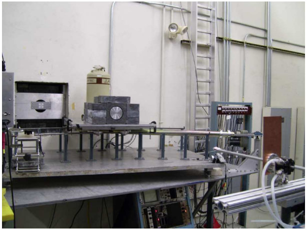

Photon-Beam Distribution

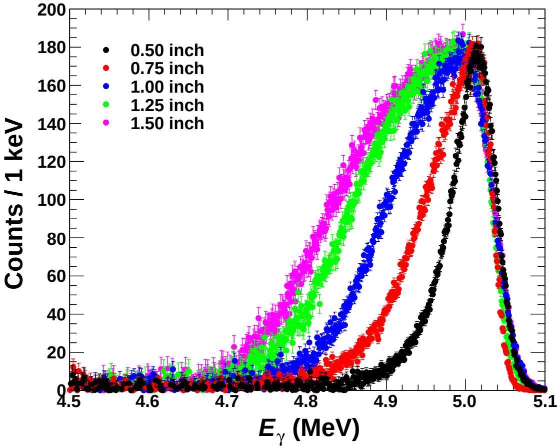

Compton scattering process:

before scattering

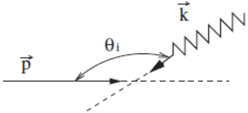

after scattering

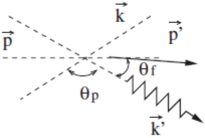

C. Sun *et al.*, Phys. Rev. ST **12**, 062801 (2009)

Branching Transitions to the Low-lying Levels in ^{90}Zr

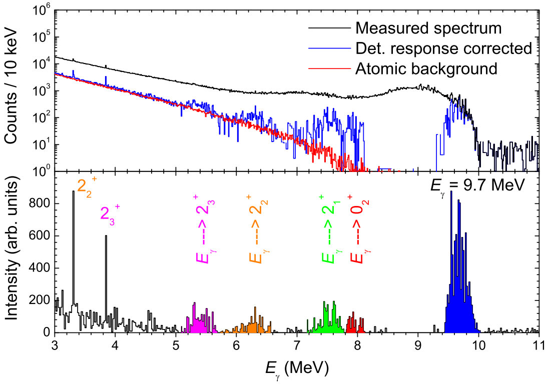

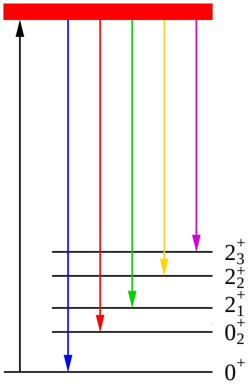

The monoenergetic beam provides separation of the ground-state transitions from the branching transitions.

Branching Transitions to the Low-lying Levels in ^{90}Zr

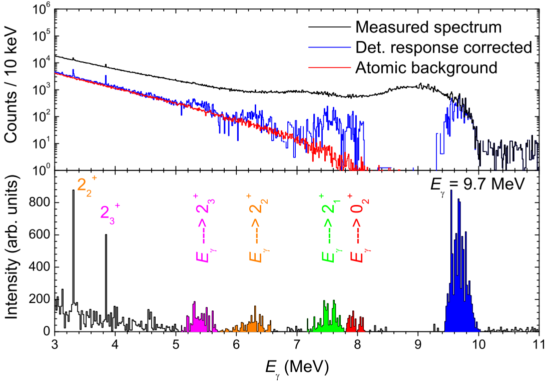

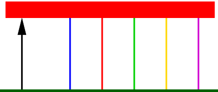

Previous work

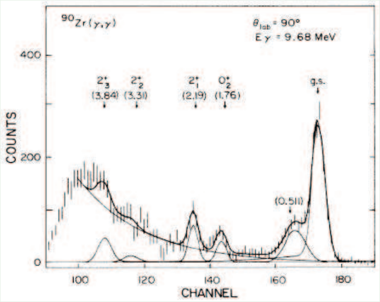

R. Alarcon *et al.*, Phys. Rev. C **36**, 954 (1987)

The monoenergetic beam provides separat
transitions from the branching transitions.

$\vec{f}_{E1}(E_\gamma) / \vec{f}_{M1}(E_\gamma)$ Ratio

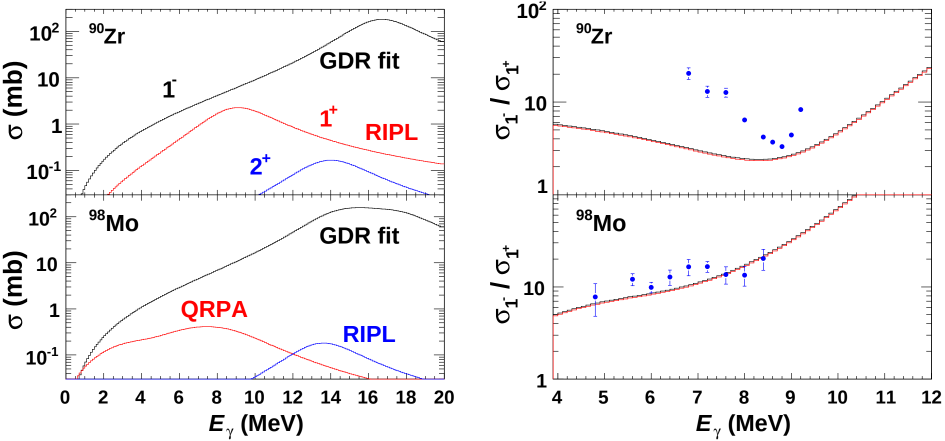

^{90}Zr: R. Schwengner *et al.*, Phys. Rev. C **78**, 064314 (2008)
^{98}Mo: G. Rusev *et al.*, Phys. Rev. C **77**, 064321 (2008)

Branching Ratios for the Ground-State Transitions

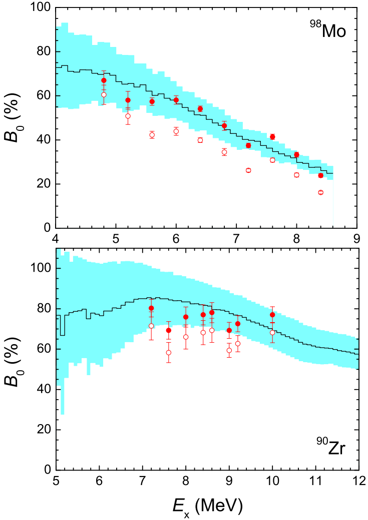

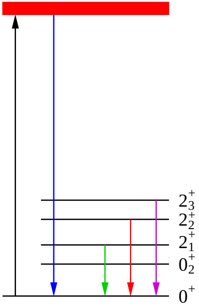

Filled circles: $B_0 = \frac{I_{g.s.}}{I_{g.s.} + I_{2_1^+} + I_{2_2^+} + I_{2_3^+}}$

Open circles: $B_0 = \frac{I_{g.s.}}{I_{g.s.} + 2I_{2_1^+} + I_{2_2^+} + I_{2_3^+}}$

No correction for bypass transitions applied!

Gamma-Ray Strength Function in ^{98}Mo

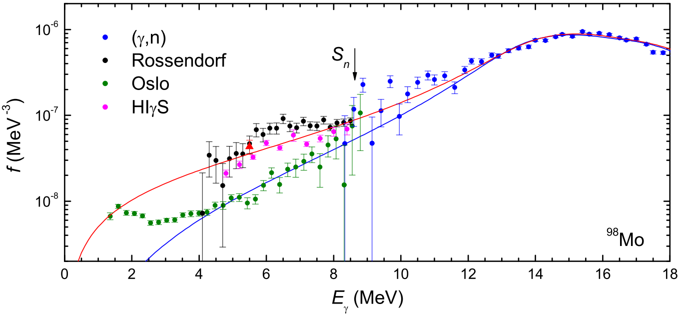

(γ, n) H. Beil *et al.*, Nucl. Phys. **A227**, 427 (1974)

(n, γ) J. Kopecky and M. Uhl, Proceedings of the NEA/ENEA and IAEA (1994)

$(^3He, ^3He'\gamma)$ M. Guttormsen *et al.*, Phys. Rev. C **71**, 044307 (2005)

(γ, γ') G. Rusev *et al.*, Phys. Rev. C **77**, 064321 (2008)

Gamma-Ray Strength Function in ^{98}Mo

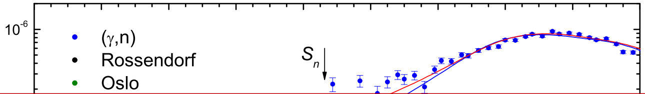

Experiments related to the $\vec{f}_{E1}\,(E_\gamma)$ in ^{98}Mo

- ^{98}Mo$(\gamma,\gamma')^{98}$Mo at HIγS
- ^{97}Mo$(n,\gamma)^{98}$Mo at the DANCE calorimeter at LANL
- ^{98}Mo$(n,n'\gamma)^{98}$Mo at TUNL

(γ, n) H. Beil *et al.*, Nucl. Phys. **A227**, 427 (1974)
(n, γ) J. Kopecky and M. Uhl, Proceedings of the NEA/ENEA and IAEA (1994)
$(^3He,^3He'\gamma)$ M. Guttormsen *et al.*, Phys. Rev. C **71**, 044307 (2005)
(γ, γ') G. Rusev *et al.*, Phys. Rev. C **77**, 064321 (2008)

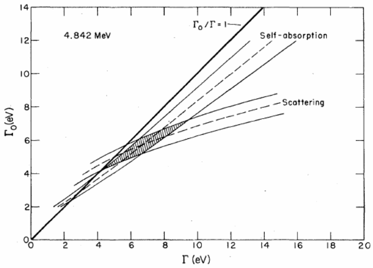

FIG. 7. Combined results of the self-absorption and scattering measurements for the 4.842 MeV level in ^{208}Pb. The dashed curves indicate combinations of Γ_0 and Γ which reproduce the experimental results; the solid curves represent the error band for each case. The shaded region contains the values of Γ_0 and Γ consistent with both experiments, and with the condition $\Gamma_0/\Gamma \leq 1$.

- photon scattering: $\frac{\Gamma_0^2}{\Gamma}$
- self absorption: $\frac{\Gamma_0}{\Gamma}$
- $\sigma_\gamma = \frac{\Gamma}{\Gamma_0}\sigma_{\gamma\gamma}$

T. Chapuran *et al.*, Phys. Rev. C **22**, 1420 (1980)

Advantage

The combination of photon-scattering and self-absorption measurements allows determination of Γ_0 and Γ in **a model (simulations) independent way!**

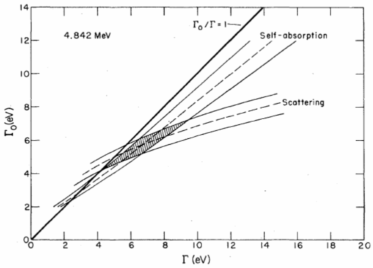

FIG. 7. Combined results of the self-absorption and scattering measurements for the 4.842 MeV level in ^{208}Pb. The dashed curves indicate combinations of Γ_0 and Γ which reproduce the experimental results; the solid curves represent the error band for each case. The shaded region contains the values of Γ_0 and Γ consistent with both experiments, and with the condition $\Gamma_0/\Gamma \leq 1$.

- photon scattering: $\frac{\Gamma_0^2}{\Gamma}$
- self absorption: $\frac{\Gamma_0}{\Gamma}$
- $\sigma_\gamma = \frac{\Gamma}{\Gamma_0}\sigma_{\gamma\gamma}$

Future experiment

PAC approved nuclear self-absorption experiment on ^{89}Y

T. Chapuran *et al.*, Phys. Rev. C **22**, 1420 (1980)

Advantage

The combination of photon-scattering and self-absorption measurements allows determination of Γ_0 and Γ in **a model (simulations) independent way!**

Dipole Strength in ^{138}Ba

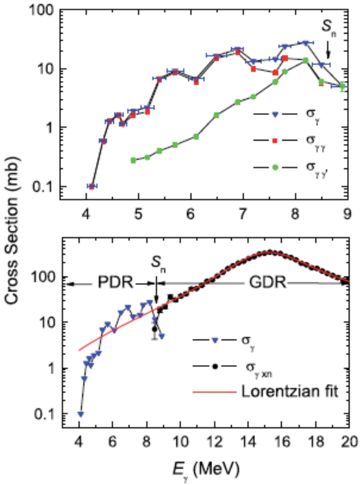

GDR tail

The GDR tail follows the extrapolation of the Lorentzian curve.

A. P. Tonchev *et al.*, Phys. Rev. Lett. **104**, 072501 (2010)

Discrete Excitations in ^{235}U

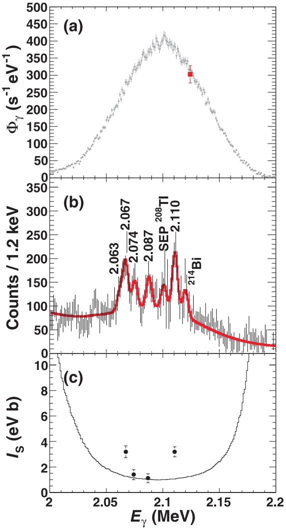

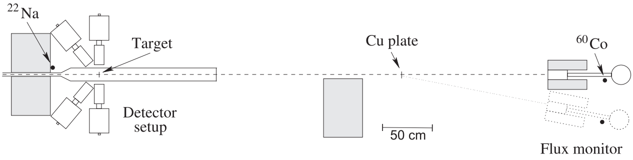

- High detection sensitivity.
- Observed 15 discrete deexcitations (12 ground-state transitions and 3 branching transitions) for the first time in the range from 1.8 to 3.0 MeV.

E. Kwan, G. Rusev *et al.*, Phys. Rev. C (2010), submitted

Elastic-Scattering Cross Section in ^{235}U

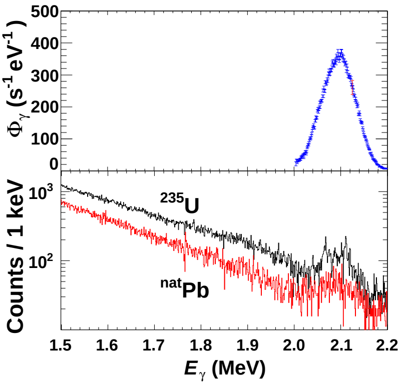

- Incoherent elastic scattering dominates above the coherent scattering.
- The intensity of the ground-state transitions is negligible than the intensity of the branching transitions.

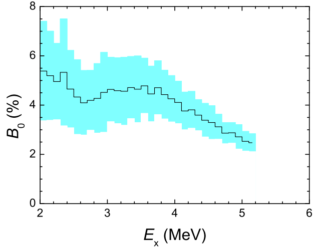

Summary

- Cascade simulations with standard assumptions for the level density (BSFG model) and strength functions (GDR fit, RPA calculations, RIPL) provide a good estimate for the branching ratios of transitions to the ground state.
- Measured ratios $\vec{f}_{E1}(E_\gamma)/\vec{f}_{M1}(E_\gamma)$ show that the $M1$ resonance in ^{90}Zr is narrower than that proposed in RIPL while the $M1$ strength in ^{98}Mo is spread over a wide energy range.
- The $E1$ strength below the neutron-separation energy follows the extrapolation of the Lorentzian fit of the GDR.
- The incoherent elastic scattering from the heavy nuclei in the actinide region dominates above the coherent scattering.

Acknowledgements

E. Kwan[1]
R. Raut
A. P. Tonchev
W. Tornow

A. S. Adekola[2]
C. T. Angell[3]
S. L. Hammond
H. J. Karwoswski

J. H. Kelley
C. Huibregse

R. Schwengner and the Nuclear Division FZD

This work was supported in part by the US Department of Energy under grants DE-FG02-97ER41033, DE-FG02-97ER41041, DE-FG02-97ER41042 and DE-FG52-09NA29448.

[1] Present address: Lawrence Livermore National Laboratory
[2] Present address: Oak Ridge National Laboratory
[3] Present address: Lawrence Berkeley National Laboratory